EARTH SURFACE PROCESSES AND LANDFORMS
Earth Surf. Process. Landforms **34**, 1811–1821 (2009)
Copyright © 2009 John Wiley & Sons, Ltd.
Published online in Wiley InterScience
(www.interscience.wiley.com) DOI: 10.1002/esp.1877

Cobble cam: grain-size measurements of sand to boulder from digital photographs and autocorrelation analyses†

Jonathan A. Warrick,[1] David M. Rubin,[1] Peter Ruggiero,[2] Jodi N. Harney,[3] Amy E. Draut[1] and Daniel Buscombe[1]
[1] US Geological Survey, Coastal and Marine Geology, Santa Cruz, CA, USA
[2] Oregon State University, Geosciences Department, Corvallis, OR, USA
[3] Coastal & Ocean Resources Inc., Sidney, BC, Canada

Received 17 December 2008; Revised 19 June 2009; Accepted 29 June 2009

Correspondence to: J.A. Warrick, US Geological Survey, Coastal and Marine Geology, Santa Cruz, CA, USA. Email: jwarrick@usgs.gov
† The contributions of Jonathan A Warrick, David M Rubin, Amy E Draut and Daniel Buscombe to this article were prepared as part of their duties as United States Federal Government Employees.

ESPL
Earth Surface Processes and Landforms

ABSTRACT: A new application of the autocorrelation grain size analysis technique for mixed to coarse sediment settings has been investigated. Photographs of sand- to boulder-sized sediment along the Elwha River delta beach were taken from approximately 1·2 m above the ground surface, and detailed grain size measurements were made from 32 of these sites for calibration and validation. Digital photographs were found to provide accurate estimates of the long and intermediate axes of the surface sediment ($r^2 > 0{\cdot}98$), but poor estimates of the short axes ($r^2 = 0{\cdot}68$), suggesting that these short axes were naturally oriented in the vertical dimension. The autocorrelation method was successfully applied resulting in total irreducible error of 14% over a range of mean grain sizes of 1 to 200 mm. Compared with reported edge and object-detection results, it is noted that the autocorrelation method presented here has lower error and can be applied to a much broader range of mean grain sizes without altering the physical set-up of the camera (~200-fold versus ~6-fold). The approach is considerably less sensitive to lighting conditions than object-detection methods, although autocorrelation estimates do improve when measures are taken to shade sediments from direct sunlight. The effects of wet and dry conditions are also evaluated and discussed. The technique provides an estimate of grain size sorting from the easily calculated autocorrelation standard error, which is correlated with the graphical standard deviation at an r^2 of 0·69. The technique is transferable to other sites when calibrated with linear corrections based on photo-based measurements, as shown by excellent grain-size analysis results ($r^2 = 0{\cdot}97$, irreducible error = 16%) from samples from the mixed grain size beaches of Kachemak Bay, Alaska. Thus, a method has been developed to measure mean grain size and sorting properties of coarse sediments. Copyright © 2009 John Wiley & Sons, Ltd.

KEYWORDS: sediment; autocorrelation; grain-size analysis; Elwha River; beach

Introduction

Grain size exerts a fundamental control on the erosion, movement and deposition of sediment particles, and can influence morphology and physical processes working on and along landforms (Klingeman and Emmett, 1982; Gomez, 1983; Mason and Coates, 2001; Rubin and Topping, 2001; Finkl, 2004; Buscombe and Masselink, 2006). Grain size varies considerably over space (e.g. bedforms and landforms) and through time at a single location thereby exerting control over physical transport and sedimentation processes. It is, therefore, important to have a means by which to accurately assess sediment grain sizes rapidly and at low cost.

Obtaining accurate grain-size data from coarse sediments can be time-consuming and challenging. For example, Kellerhals and Bray (1971) and Adams (1979) note that a recommended sample mass for statistically acceptable sieve analysis of cobble would range from tens to hundreds of kilograms depending on grain size. Obviously it would be exceptionally difficult to obtain, transport, and process numerous samples of such size from most landforms of interest. More traditional methods, such as pebble counts (Wolman, 1954; Leopold, 1970), are appropriate for characterizing grain size distributions of landforms, but the field time required for this style of data collection can be prohibitive. One standard pebble count sample of 100 clasts can take a single operator between 10 min and 1 h depending on the number of axes and style of measurement.

To alleviate these problems, a number of researchers have investigated the use of remotely sensed imagery to measure grain size. For example, Kellerhals and Bray (1971) and Adams (1979) compared photograph and sieve data from coarse-grained river bars and beaches and found that mean grain sizes from photographs and sieving were directly comparable with a slight negative bias resulting from partial burial of rocks. More recently, Butler *et al*. (2000), Sime and Ferguson (2003), Rubin (2004), Carbonneau *et al*. (2004), and Graham *et al*. (2005a) have developed digital image processing techniques

– summarized below – to provide measures of grain-size properties in digital photographs. These techniques have been applied to imagery collected with ground-based photography (Butler *et al.*, 2000; Graham *et al.*, 2005a; Barnard *et al.*, 2007), airborne photography (Carbonneau *et al.*, 2004; Verdu *et al.*, 2005), and underwater photography (Chezar and Rubin, 2004; Rubin, 2004; Rubin *et al.*, 2007).

The goal of this study was to develop a data collection and analysis technique to rapidly collect and process mean grain-size samples from the broadest distribution of grain sizes (sand to boulder) and in a manner that was as time-efficient and cost-effective as possible. Our intention was not to develop a method that supersedes existing methods, rather we sought to develop an efficient and accurate method that could be used in conjunction with other methods, when appropriate, and to characterize grain sizes over many different spatial scales. Thus, the purpose of this study is to provide a technique that could be used to rapidly characterize grain sizes of remote sites with acceptable levels of accuracy. We use the mixed-sediment beach of the Elwha River delta (Warrick *et al.*, 2009) for method development and application, and demonstrate its potential transferability with an assessment of a mixed-sediment beach of Kachemak Bay, Alaska.

Photographic techniques for grain size measurements

Photographic methods have long been used to characterize coarse sediment owing to the rapidity of field data collection and short analysis time. The basic method is to obtain a high-resolution photograph of the ground surface, subsample and/or preprocess the photograph, if necessary, and assess the grain size in the image using the known ground scale and either a user- or computer-based measurement tool. As discussed below, a number of grain size measurement tools exist.

Although photographic techniques for grain-size analysis have been developed and applied to many geomorphic settings, it is important to note that a number of limitations exist for this style of data collection. First, photo sampling can characterize only the exposed surface, which may or may not be related to subsurface sediment properties (Church *et al.*, 1987). On a similar note, photos only provide planar, not volumetric, samples. Thus, only two dimensions of each clast can be measured in the photograph as opposed to the three dimensions of actual sediment (e.g. Ibbeken and Schleyer, 1986). Photos cannot provide direct volume-by-weight samples such as provided by sieving, although Kellerhals and Bray (1971) and Church *et al.* (1987) have shown that grid-by-number counts from photos are related to these volumetric metrics for homogeneous sediment distributions. There is also the potential for bias in these methods, especially if certain particles cannot be properly observed in the photo owing to imbrication, lighting effects and shadowing, and/or the upper or lower spatial resolution of the image (cf. Adams, 1979). Lastly, no physical sample will exist following the field program, which prevents post-sampling analyses of three-dimensional shape, mineralogy, chemistry, or other properties of the sediment.

Despite these limitations, many studies have used photographic methods successfully to meet monitoring goals. Early method development utilized traditional film cameras and manual counts of the sediment sizes in photograph prints (Kellerhals and Bray, 1971; Iriondo, 1972; Adams, 1979). Digital methods were first developed by Ibbeken and Schleyer (1986), who used digital scans of the photos with digitizing programs to trace all exposed clasts. Although these user-based techniques require approximately an hour per sample for analysis (i.e. approximately the same amounts of time as traditional pebble counts), they do provide accurate measures of the grain size distribution and are still used for calibrating the more fully digital methods summarized below (Graham *et al.*, 2005a; Barnard *et al.*, 2007).

Digital analysis methods can be grouped into two general types: those that attempt to characterize and measure the individual clasts, and those that use empirical relationships of image properties and grain size (Buscombe and Masselink, 2009). The former method has been developed through the work of Butler *et al.* (2001), Sime and Ferguson (2003), and Graham *et al.* (2005a,b), with the goal of using image processing techniques to identify, segregate and measure the dimensions of each individual clast in the image. One significant challenge of this approach is the recognition of and/or correction for partially concealed grains. These techniques have been applied successfully and have been shown to provide accurate estimates of the particle size distributions above a certain size threshold when compared with physical samples (Graham *et al.*, 2005a). These techniques were developed for hand-held or pod-mounted cameras and one grain-size analysis per photo, and one version (Graham *et al.*, 2005a) is currently available commercially (Sedimetrics, 2008). Other limitations to these methods include the lower limit of clast detection at approximately 23 pixels and the need for carefully controlled lighting (Graham *et al.*, 2005a).

The empirical methods have utilized statistical measurements of the photograph texture (see review by Carbonneau *et al.*, 2004) to infer grain size properties. Texture is quantified using spatial statistics of image pixel brightness, and the two current techniques include: (1) local semivariance, used to characterize grain size variations from airborne imagery of landforms such as gravel bars (Carbonneau *et al.*, 2004; Verdu *et al.*, 2005), and (2) autocorrelation (Rubin, 2004). The autocorrelation technique was originally developed to better characterize sand distributions from underwater photos using the rate of autocorrelation decrease with increasing pixel shifts. This technique has been shown to work on both single images and in one-dimensional profiles of images (Rubin, 2004), and there have been recent successes in evaluating grain-size distributions with these methods (Buscombe, 2008). Both of the empirical techniques benefit from not needing to detect individual clast boundaries in the images, resulting in low minimum size thresholds (as low as 2–3 pixels; Rubin, 2004) and accurate grain size characterization over approximately two orders-of-magnitude of grain diameters.

Here we evaluate a new application of the autocorrelation technique to mean grain sizes of coarse-grained landforms, such as mixed beaches and gravel bars. This technique was chosen because of the highly accurate results of previous work, free access to autocorrelation computer coding, and the potential for application over broad ranges of grain size.

Methods

Study sites

We chose to develop and apply a grain size analysis method for the beaches of the Elwha River delta of the Olympic Penninsula of Washington, USA (Figure 1), because of the mixed grain sizes encountered and a pending dam removal project that should alter river supplies of sediment to the beach. The morphology and historical change of the delta shoreline has been studied and synthesized by Warrick *et al.* (2009), so only the physical setting is described briefly here.

Copyright © 2009 John Wiley & Sons, Ltd.

DOI: 10.1002/esp

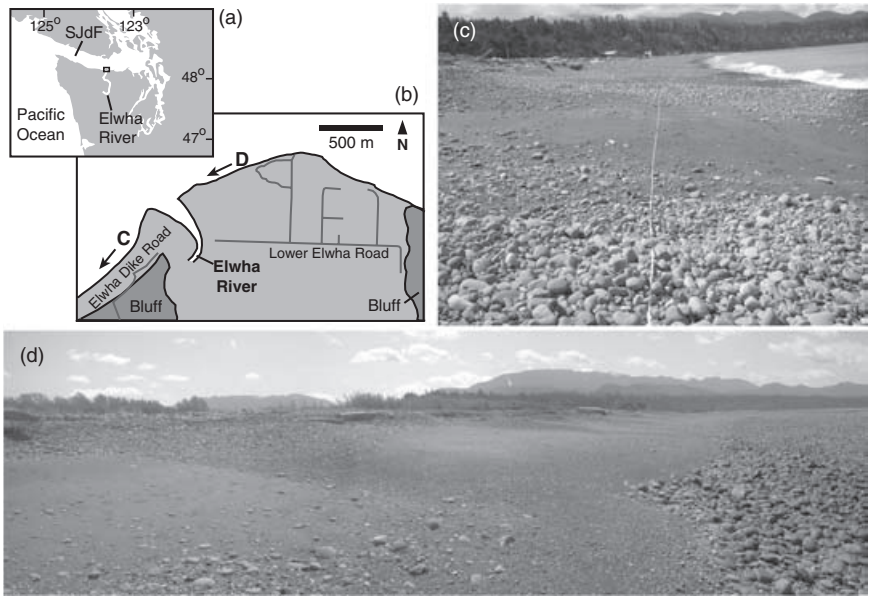

Figure 1. Location and sediment characteristics of the Elwha River delta beach. (a) Regional map showing the Elwha River, the Strait of Juan de Fuca (SJdF), and the inset box for (b). (b) The Elwha River delta including the location and field–of–view directions of the photographs shown in (c) and (d).

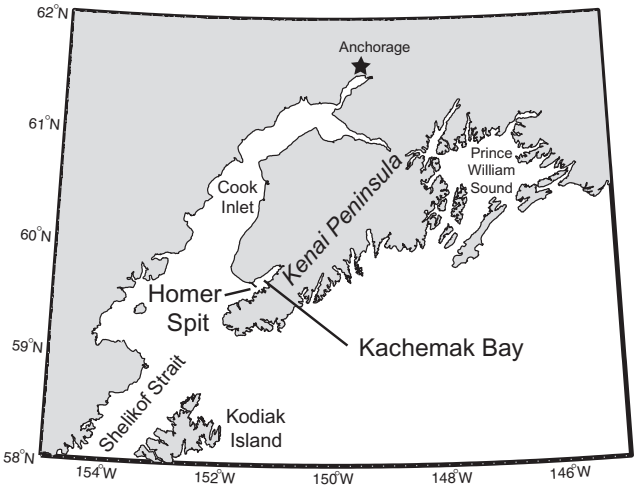

Figure 2. Location of Homer Spit in Kachemak Bay, Alaska, where sediment data were collected as summarized in the text and by Ruggiero *et al*. (2007).

The beaches are mixed grain size, sand to boulder, and differ on either side of the river mouth bar. West of the river mouth the beach is steep, reflective and cuspate (Figure 1c). The beach east of the river mouth has a reflective foreshore and a dissipative, cobble low-tide terrace (Figure 1d). These differences are thought to be caused by geomorphic adjustment produced by sediment flux decreases related to the river's dams.

Sediment flux will be restored to the delta following a pending dam removal, which may reduce or reverse shoreline erosion trends of the past and change the grain-size distribution found in the river and on the beach (Randle *et al*., 1996). Accurate grain size information is needed, therefore, to track the coastal and fluvial responses to the restoration.

We evaluate the transferability of the technique developed in this paper to the mixed-sediment beaches located along Homer Spit of the north shore of Kachemak Bay, Alaska (Adams *et al*., 2007; Figure 2). The tectonically active, megatidal (spring tide range greater than 8 m), and wave-dominated beaches of Kachemak Bay provide an ideal natural laboratory

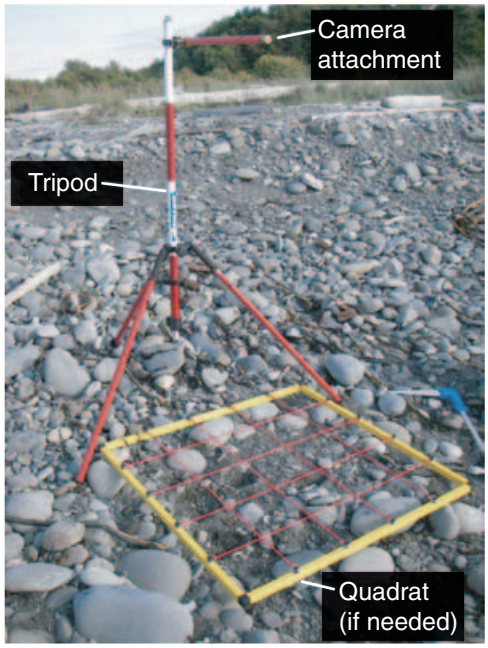

Figure 3. Tripod set–up for obtaining digital photographs of surface sediment.

for investigating mixed sediment beach processes. Surficial sediments range from fine sand to boulders and the morphodynamics of these beaches include self-organized bedforms composed of fine-to-medium sand that migrate as coherent packages over a mobile coarse substrate (Ruggiero *et al*., 2007).

Photo collection and analysis

Photographs were obtained from a Cannon Powershot S3 IS 5·9-megapixel (2816 by 2112 pixels) digital camera held steady using a camera attachment from a survey tripod (Figure 3). The camera attachment was adjusted so that an image was taken orthogonal to, and at approximately 1·2 m above, the ground surface. A delay timer was used to avoid camera shake

Copyright © 2009 John Wiley & Sons, Ltd.

DOI: 10.1002/esp

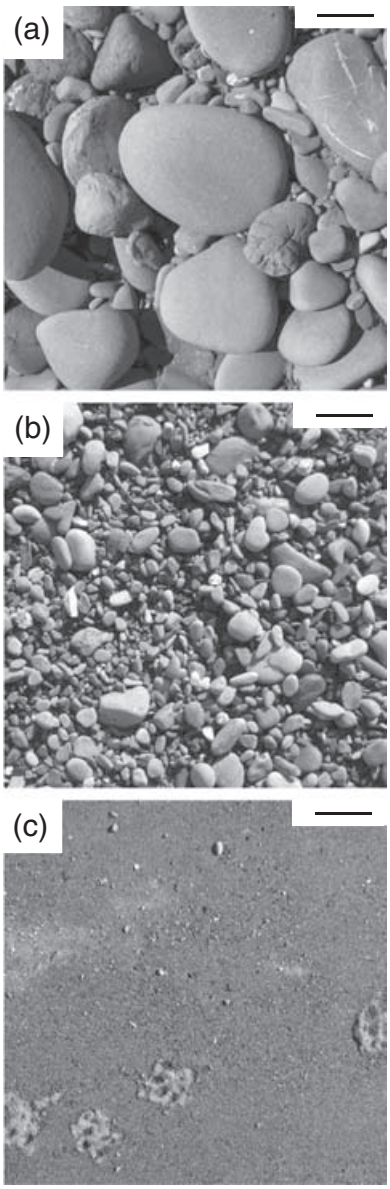

Figure 4. Example digital photographs of beach sediment taken from a tripod 1·2 m from the ground surface. The scale bar in each photo represents 100 mm.

during image collection. A tape measure was placed in the field-of-view of all photographs near the tripod legs for ground scale. The image resolution varied between photos because modifications to the tripod were often necessary to obtain images that were orthogonal to the ground and without shadows cast from the apparatus. These modifications resulted in variations in camera heights of approximately ± 0·2 m, resulting in image resolutions of approximately 0·3 mm/pixel in all photos.

For calibration and verification of the autocorrelation method, we sampled 32 sites across all the major sizes and distributions of sediment observed along the Elwha beach (Figure 4). The primary purpose of these sites was to develop and evaluate calibration curves for the autocorrelation technique as described below. Grain size distribution data was generated for each digital photograph using the following grid-by-number technique. A regular spaced (200-pixel) digital grid was projected on the photograph producing a 9-by-12 matrix (i.e. 108 samples) using the Adobe Photoshop computer application. For the clast underlying each grid intersection, the longest exposed length and the associated orthogonal length were measured in pixels using a line-drawing tool. These measurements are subsequently termed the major and minor axis diameters from the photographs (P_M and P_m, respectively). If there was no distinguishable clast under the grid point, the rock directly up and to the left was measured. Notes were made if the clast was partly buried (<50% of rock perimeter buried), mostly buried (>50% of perimeter buried), and/or partially outside the photograph field of view. Rocks that were too small to be measured with the resolution of the photograph (typically 3–4 pixel length, ~1·2 mm long) were defined to be 'sand' and given an arbitrary grain-size of 2 pixels (~0·6 mm). Length measurements in pixels were converted to linear distances with the ground scale.

Grain-size distribution statistics for each photograph were calculated from the 108 rock samples unless any of the sampled rocks lay off the photograph. In this case, the entire row or column of samples with the off-image rock was removed from the statistical calculations, consistent with the methodology of Adams (1979). Grain size statistics calculated for each photo included: mean, median (D_{50}), standard deviation, various percentiles (D_{95}, D_{84}, D_{16} , D_5), the graphical mean ((D_{84} + D_{16} + D_{84}) / 3), and the graphic standard deviation (herein defined as the 'sorting index' and equivalent to (D_{84} – D_{16}) / 4 + (D_{95} – D_5) / 6·6). These grain size statistics were calculated on both a linear and logarithmic (phi) basis for both the longest and shortest axes observed. Further, these statistics were also computed for all clasts measured and for only those clasts observed to be fully exposed. Below we show that the optimal results occurred for the linear-based grain sizes computed without the buried clasts.

A secondary purpose of the 32 grain-size samples was an evaluation of the relationship between photograph and actual measurements of grain size. For this analysis 16 clasts were identified in each sample using a quadrat (Figure 3). The 16 clasts were then marked with ink for ease of locating in subsequent measurements and a second photograph was taken. The photographic measurements were made of the longest axis and its orthogonal from these clasts using a drawing tool in Adobe Photoshop (P_M, P_m). Once the second photograph was obtained, each clast was removed from the ground surface and measured for long, intermediate, and short axis lengths (F_L, F_I, F_S) – all orthogonal to each other – with either 40-cm or 15-cm calipers, depending on clast size. Comparisons between the two photograph axes (P_M, P_m) and the three field axes (F_L, F_I, F_S) were conducted with linear regression with the goal of evaluating the relationship between photo-based and field-based measurements of sediment.

Photographic sampling was also conducted to evaluate the effects of environmental conditions on the autocorrelation results. To evaluate the effects of ground surface wetness, we obtained digital photographs in dry sediment of various sizes and then completely wetted the sediment within the field of view with a gardening water pail without moving or disturbing the camera or the exposed sediment on the ground surface. We also obtained a number of images of sediment that had patchiness in surface wetness to evaluate the effects on the grain-size results.

The effect of ambient lighting was evaluated by leaving the camera set-up for a complete day over a body of cobbles. Photographs were obtained every 1·5 h using a number of methods: (1) ambient solar lighting only; (2) ambient lighting with camera flash; (3) shaded with no flash; and (4) shaded with camera flash. Shading for this experiment was provided by a 1·3 m diameter umbrella placed between the sun and the ground surface.

Copyright © 2009 John Wiley & Sons, Ltd.

DOI: 10.1002/esp

Photographs were obtained also over the two representative beach landforms shown in Figure 1c and d to evaluate the applicability of our technique for characterizing grain-size variations in the field. Sample locations and elevations were measured using a real-time kinematic differential global positioning system (RTK-DGPS), which has an accuracy of approximately ±100 mm in both the horizontal and vertical at this site (Warrick *et al*., 2007). We also noted the time required to collect and process the photographs to assist with future activities.

Lastly, photos were obtained from the beaches of Kachamak, Alaska to evaluate the transferability of the technique to other sites. Eleven photographs were taken in the same manner as described above. Photo-based grain size measurements were evaluated using the same grid-by-number techniques discussed above, which were compared with autocorrelation results using linear regression.

Autocorrelation analyses

All photographic images were evaluated by or used in the autocorrelation analysis technique. The main purpose of this section is to identify the main characteristics of our method and to note how our method differs from the former applications of the autocorrelation technique. We note that details of the autocorrelation technique and computer coding can be found in Rubin (2004) and Barnard *et al*. (2007), and these techniques are evaluated in some detail by Buscombe and Masselink (2009). Fundamentally, the autocorrelation statistic is used to evaluate the spatial scales of image contrast (i.e. texture), which is a primary function of grain size (Figure 4). Autocorrelation (i.e. the correlation of something with itself) will decrease monotonically as pixels are shifted away from the original pixels, and the rate of autocorrelation decrease is inversely proportional to grain size (Figure 5). Thus the goal of autocorrelation grain size analyses is to find autocorrelation curves (such as shown in Figure 5) that are representative of specific grain sizes for the sediment of interest, so that these curves can be used to calibrate other photos with unknown grain size.

We developed calibration curves from best-sorted samples from the 32 intensely sampled sites. A total of 13 samples were combined to produce seven calibration curves ranging in mean grain size from 3 to 630 pixels. The sorting index for these 13 samples averaged 0·70ϕ (moderately well sorted), with a standard deviation of 0·19ϕ. Three of the final curves (76, 133, and 221 pixels) were derived from averaging multiple samples into a single curve, for which the grain size was set equal to the mean of the samples, consistent with previous applications (e.g. Barnard *et al*., 2007). The remaining 19 samples, which ranged in mean grain size from 12·7 to 225 pixels (4 to 117 mm) and sorting indexes from 0·69ϕ to 2·52ϕ (moderately well sorted to very poorly sorted), respectively, were used to optimize the method and compute uncertainty.

The autocorrelation analysis was then conducted on images by calculating a correlation coefficient (r) for each pixel shift, and interpolating each of these r into the set of calibration curves to calculate grain size in pixels. This analysis was conducted twice by shifting images in the photograph's horizontal and vertical directions. The average of this series was deemed the mean grain size of the image, and the standard error (standard deviation normalized by the mean) of the series was calculated to compare with grain size sorting properties as discussed below. Rather than allowing this analysis to extend over the complete range of pixel shift values, we evaluated termination of the analysis once the correlation coefficient became less than a cut-off value. The best solution for the cut-off correlation coefficient was determined by minimizing analysis error from the set of 19 samples. Grain size analyses were conducted in units of pixels, and these results were converted into units of length using the ground scale of each photograph.

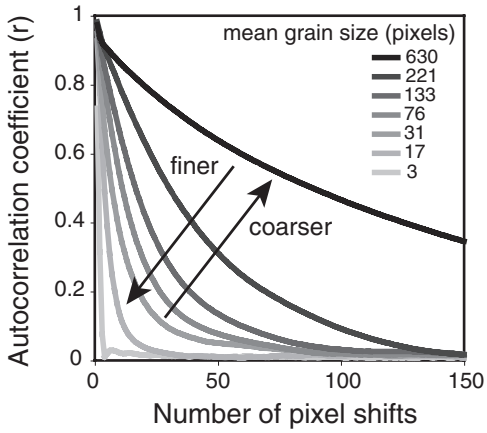

Figure 5. Relationship between pixel shifts and autocorrelation coefficient for photographs of Elwha River delta sediment with different mean grain size, represented by the mean minor-axis length (P_m) in pixels of the unburied sediment.

Results

Comparison of photograph and field measurements

The measurements of grain size from the photos and in the field provided consistent estimates of the clast axes lengths (Figure 6). Excellent linear regression was found for comparison of the longest axes in both methods (P_M versus F_L; Figure 6a) and for comparison of the minor axes in the photo (P_m) with the actual intermediate axes (F_I; Figure 6b). This, coupled with the poor correlation between photographic measurement axes and the actual short axes (F_S; Figure 6c), suggests that clasts on the beach are dominantly oriented with the short axes (i.e. F_S) in the vertical dimension. Hence, the photos provide excellent estimates of the actual long and intermediate axes of the clasts, the latter of which will be used throughout this paper to calculate grain-size distribution statistics owing to the common use of the intermediate axis for grain size analyses (Church *et al*., 1987). Mean error in using P_m to estimate F_I was calculated on the basis of percentage, linear distance, and logarithmic distance to be –11%, –6·0 mm, and 0·19ϕ, respectively, and the linear regression between these variables was found to be:

$$P_m = 0.96F_I - 2.9 \quad (1)$$

Autocorrelation optimization

Autocorrelation calibration curves were derived from the well to moderately well sorted samples. Note that the autocorrelation calibration curves (cf. Figure 5) were very similar to exponential functions ($r^2 = 0{\cdot}97$ to $0{\cdot}99$). Assuming that mean grain size exerted a primary control on the autocorrelation relationship, one would expect a relationship such that

Copyright © 2009 John Wiley & Sons, Ltd.

DOI: 10.1002/esp

$$r(x) = \exp(-kx) \quad (2)$$

where $r(x)$ is the correlation coefficient at pixel step x, and k is an exponential decay coefficient, which would be related to the grain size (z) such that $k \sim z^{-1}$. Using these simple assumptions and the best-fit k from the calibration curves, we found that k was equivalent to:

$$k = (0.19z + 2.6)^{-1} \quad (r^2 = 0.99) \quad (3)$$

This suggests that mean grain size exerted primary control on the texture of photographs from these natural sediments, and that exponential autocorrelation properties may be inherently and systematically related to grain size.

Applying the calibration curves to the 19 remaining samples, optimal results were found for a correlation coefficient cut-off threshold of 0·25 (Figure 7). For this cut-off value the linear regression correlation between the actual and estimated grain size was a maximum of 0·93 and the r.m.s.e. of these data was a minimum of 19%. Using this analysis, grain sizes were estimated fairly accurately, and errors were normally distributed (Figure 8). The mean error was 13% (Figure 8b), which suggests a slight overprediction of the photo-measured grain sizes. This is consistent with the linear regression lying above the 1 : 1 line (Figure 8a). The irreducible error (e_i) is the r.m.s.e. (e_{rms}) that cannot be accounted for by this mean error (e_m) and can be computed by (cf. Graham *et al.*, 2005a):

$$e_i = \left[e_{rms}^{\ 2} - e_m^{\ 2}\right]^{0.5} \quad (4)$$

The irreducible error for our analysis was computed to be 14% (Figure 8b).

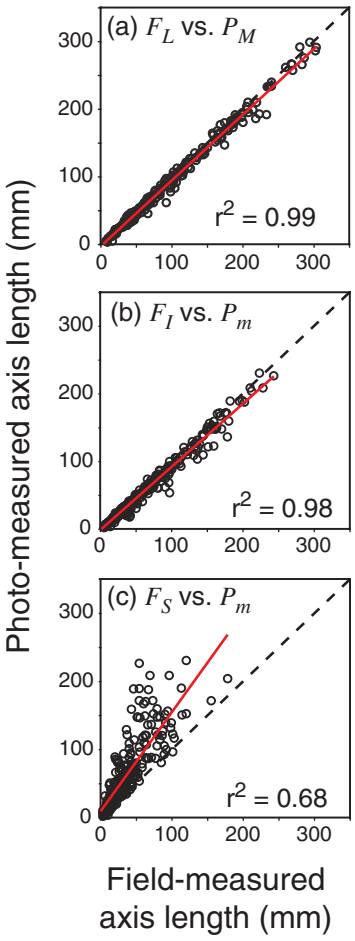

Figure 6. Comparisons of field (F) and photograph (P) measurements of unburied Elwha River delta sediment axis diameters. For the field data, L = long, I = intermediate, and S = short axes, whereas for the photograph data, M = major and m = minor axes. The 1 : 1 relationship is shown with a dashed line, and the least squares, linear regression is shown with a red solid line. Photographs provide good estimates of the long and intermediate axes as shown in (a) and (b), but relatively poor estimates of the short axis (c). Analysis based on 255 samples from 31 sites.

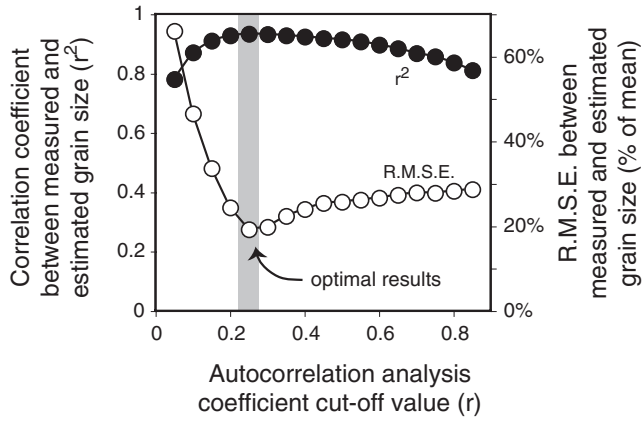

Figure 7. Effect of the autocorrelation analysis coefficient cut–off value on the regression between measured and estimated mean grain size. Optimal results (highest correlation, lowest error) occurs for a cut–off autocorrelation value of 0·25.

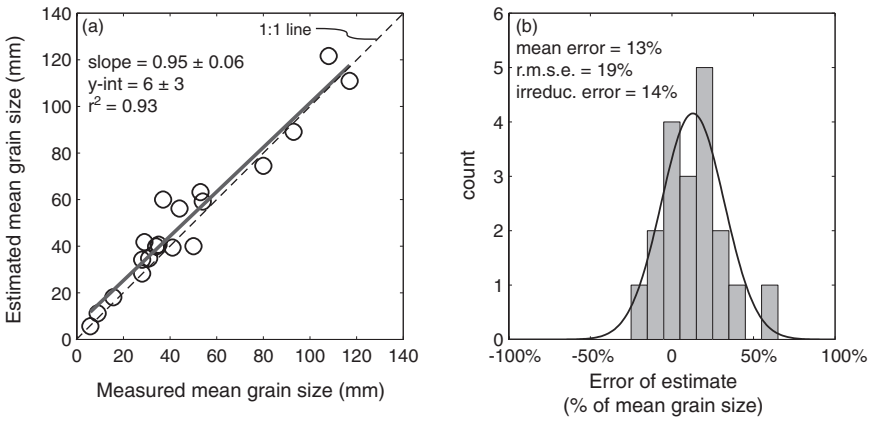

Figure 8. Comparison of the measured and estimated mean grain size from the optimized autocorrelation method: (a) comparison with linear regression statistics, (b) histogram of the error of the estimates. Solid line in (b) is a normal distribution calculated with estimate errors.

Copyright © 2009 John Wiley & Sons, Ltd.

DOI: 10.1002/esp

Note that these percentage errors were not related to grain size or the sorting index (both $r^2 < 0{\cdot}04$). We conducted analyses for both ϕ- and linear-based measurements of the mean and median grain size and found highest correlation and least r.m.s.e. for the mean grain size in linear units. Thus, the optimal results were found for analyses of the mean grain size using an analysis cut-off autocorrelation coefficient of 0·25, which produced r.m.s.e. of 19% and 14% irreducible error, the difference related to overprediction ($e_m > 0$; Equation (4)). Including this error with the underpredction errors of the field-to-photo analyses discussed earlier, the total mean predictive error of autocorrelation for ground-based measurements of mean, intermediate clast axes is thus ~2%. This total predictive error was corrected for by a linear correction factor of 1·02 in the results presented later.

Sediment sorting

Sediment sorting of each sample was measured by the graphical standard deviation (i.e. the 'sorting index'), which, as noted above, did not correlate with estimate errors for the photos ($r^2 < 0{\cdot}04$). However, sediment sorting was found to correlate with the standard error of the series of grain size results from all pixel shifts (power law, $r^2 = 0{\cdot}69$; Figure 9a). We explain this pattern by focusing on two samples (shown as A and B in Figure 9) with significantly different sorting properties. The moderately well sorted sample (A) has an autocorrelation coefficient (r) curve that closely resembles the exponential decay patterns of the calibration curves (Figure 9b). This close resemblance results in only 12% standard error in the series of grain size estimates from the analysis. Sample B is very poorly sorted and has an autocorrelation coefficient curve that crosses many of the calibration curves, thus deviating significantly from their exponential-like shapes (Figure 9b). This results in a much higher standard error of the series of grain size estimates (standard error is 50%; Figure 9a). This measure of curve fit – the standard error of the estimate – is by no means a perfect predictor of grain size sorting, but it does explain much more that half of the variance in the sorting data, and the r.m.s. error of this sorting estimate is less than 0·5ϕ. Thus, although sediment sorting was not found to influence the accuracy of the mean grain-size analysis, it does influence the shape of the autocorrelation coefficient curves, which in turn is related to an easily calculated parameter, the standard error of the series of estimates. This parameter may be used to estimate sample sorting with reasonable accuracy.

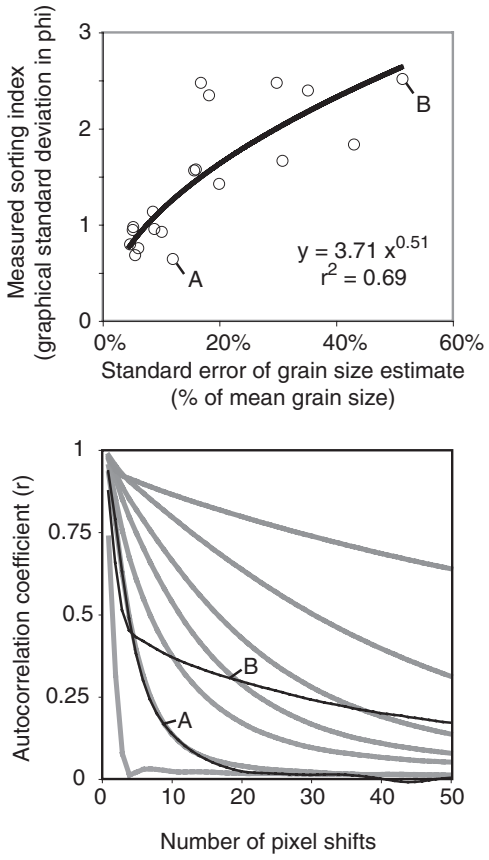

Figure 9. Effects of grain size distribution on autocorrelation results. (a) Relationship between the standard error of the autocorrelation calibration curve fit and the sorting index (*SI*). Example samples identified by A and B are shown in (b). (b) Two end members of grain size sorting and autocorrelation fit (black lines) shown with calibration curves (gray lines). Sample A is moderately well–sorted (*SI* = 0·65) and fits well to calibration curves. Sample B is very poorly sorted (*SI* = 2·52) and crosses many of the curves.

Wet–dry effects

A comparison of the ten samples obtained under identical camera set-ups but with naturally-dry and artificially-wetted conditions shows little difference in the results (Figure 10). Although the color and light-reflections in each photo were different, we found that wet samples resulted in a very subtle overprediction (mean error = 5%) of the dry samples. The irreducible error of this analysis (9%; Figure 10) was less than that found for the entire method (14%; Figure 7).

Patchiness in the wetness was found to induce significant bias, however. An example of this for coarse sand is shown in Figure 11. This photograph was subsampled into four equal area sections consisting of 500 by 500 pixels. Autocorrelation analyses were conducted on each subsample, the full image, and on regions manually chosen to be entirely wet and dry. Subsamples that were in regions continuously wet or dry consistently resulted in mean grain sizes of ~1·4 mm (Figure 11). The patchy areas, including the full image, resulted in grain sizes that were 21 to 57% higher (i.e. 1·7 to 2·2 mm) than these values. Note that these errors are in excess of the 14% error of the analysis reported above (cf. Figure 8), suggesting that the wet–dry patterns in texture significantly biased the results, resulting in significant overprediction.

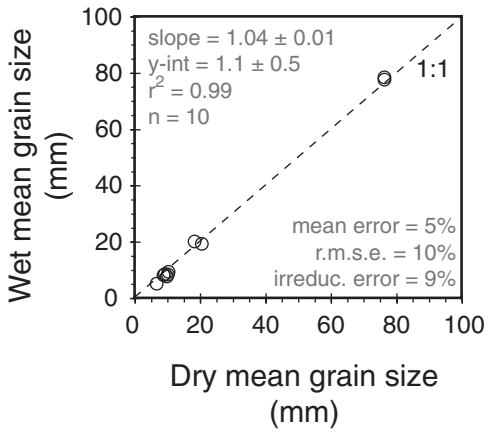

Figure 10. Comparison of autocorrelation–derived mean grain size from repeat photographs during dry (initial) conditions and artificially wetted conditions.

Copyright © 2009 John Wiley & Sons, Ltd.

DOI: 10.1002/esp

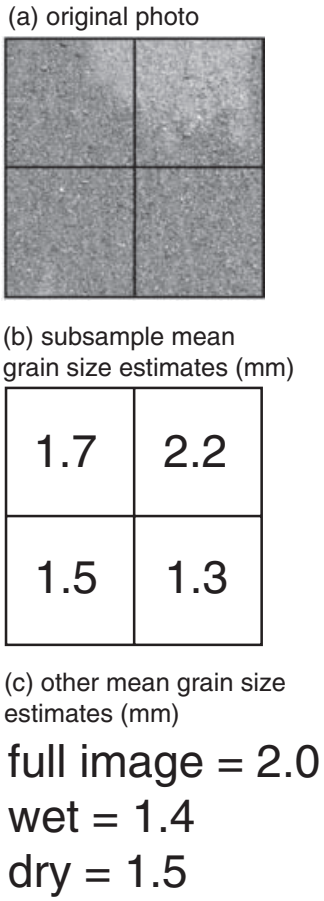

Figure 11. Example of a photograph with patchy wetness conditions, and the effects of these conditions on autocorrelation results. (a) Example photograph with four subsections delineated. (b) Autocorrelation estimates of the mean grain sizes for each of the four subsections. (c) Other mean grain–size estimates from the image samples (see text).

Lighting effects

Illumination of the photograph was found to influence the results of the autocorrelation method, and the greatest errors were associated with using ambient solar lighting (Figure 12). For a site with a mean grain size of 36 mm, ambient solar lighting could account for an r.m.s.e. of 4 mm, or ~10%, with a maximum range in the results of 9 mm. Shading the ground surface from the sun, in contrast, resulted in errors (2 mm or 5% error) that were half of the ambient lighting errors. Use of the camera flash did not alter these results significantly (data not shown). Ambient solar lighting produced results that were inversely correlated with the solar zenith angle, resulting in grain size estimates that were over-estimated when the zenith angles were low – and shadows were long – and under-estimated when zenith angles were high around midday (Figure 12). For comparison, note that the calibration and validation data and the example applications of the method were all collected under ambient solar lighting conditions without shading or flash.

Example applications of the method

Two example applications of the method are shown from the Elwha River delta beach. First, topography and photographs were taken every 1 m along four transects (A–D) across a

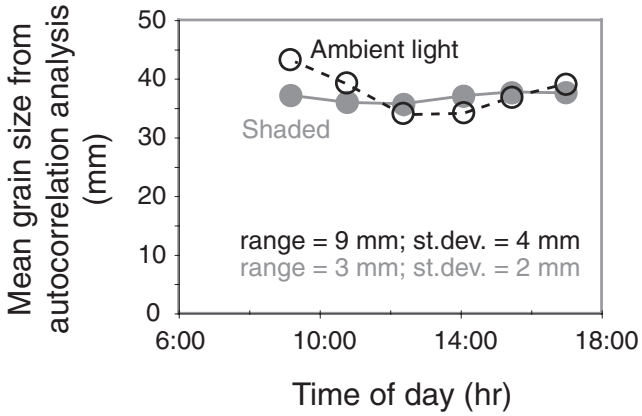

Figure 12. Effect of solar illumination angle on autocorrelation results. A site was sampled during a sunny day in both ambient light (black unfilled symbols and text) and shaded with an umbrella (gray filled symbols and text).

single beach cusp (Figure 13). The tape measure that defined transect B–B′ is shown in Figure 1c. The topography reveals cusp horns (or highs) at either end of the transects and an embayment in the center (Figure 13a). Grain size from photographs reveal that the lower portion of the embayment was sand to granules (1 to 5 mm), while the horns and upper cusp were dominated by cobble (55 to 160 mm; Figure 13b). There are also gradients in grain size between the sand and cobble end members (Figure 13b). These results are consistent with observations made during the data collection and span over two orders of magnitude of grain sizes, which far exceeds the 14% uncertainty in the analyses reported above. It took 1·5 h for two people to collect the 128 topography and grain size samples and associated field notes (i.e. 1·4 samples min^{-1}) once we were at the site with operational RTK-DGPS.

The second example of grain size data collection comes from a single cross-shore transect across the foreshore and low-tide terrace of the beach type shown in Figure 1d. For this site, data were collected every 1 m from the upper foreshore through the low-tide terrace transition, and then every 4 m on the low-tide terrace (Figure 14). Measured grain size patterns are consistent with the patterns observed at the site; the foreshore is the steepest section of the beach (tan(slope) ~ 1 : 7) with mean grain sizes ranging from 1·8 to 47·5 mm and a mean and standard deviation of 13 ± 14·5 mm. The finest sediment, which is coarse sand, appears to occur in the middle foreshore (Figure 14). The low-tide terrace, in contrast, is much less steep (tan(slope) ~ 1 : 50) and the grain sizes are significantly coarser (range = 88 to 206 mm; mean ± st.dev. = 127 ± 32 mm). Here again, the variation in the results vastly exceeds the uncertainty of the analysis. For this site, we note that it took two people approximately 20 min to collect the 30 data points and supporting notes.

Method transferability

We illustrate the potential for transferability of this technique with an application to the mixed-sediment beaches of the north shore of Kachemak Bay in the town of Homer, Alaska (Figure 2). In summer 2005 we collected 11 photographs for which both photo-based and physical measurements of grain size were conducted (Ruggiero *et al.*, 2007). Ruggiero *et al.* (2007) found strong agreements between photographic and physical measurements of exposed clasts (r^2 = 0·97), which is

Copyright © 2009 John Wiley & Sons, Ltd.

DOI: 10.1002/esp

consistent with the results from the Elwha River delta beach shown earlier. However, it is also noted that the samples were obtained at high latitude with direct solar illumination, and thus the samples included long shadows. These samples were also obtained in the intertidal region, and thus were partially wet when photographed. With these conditions and the results presented, we should expect overprediction of grain-size estimates.

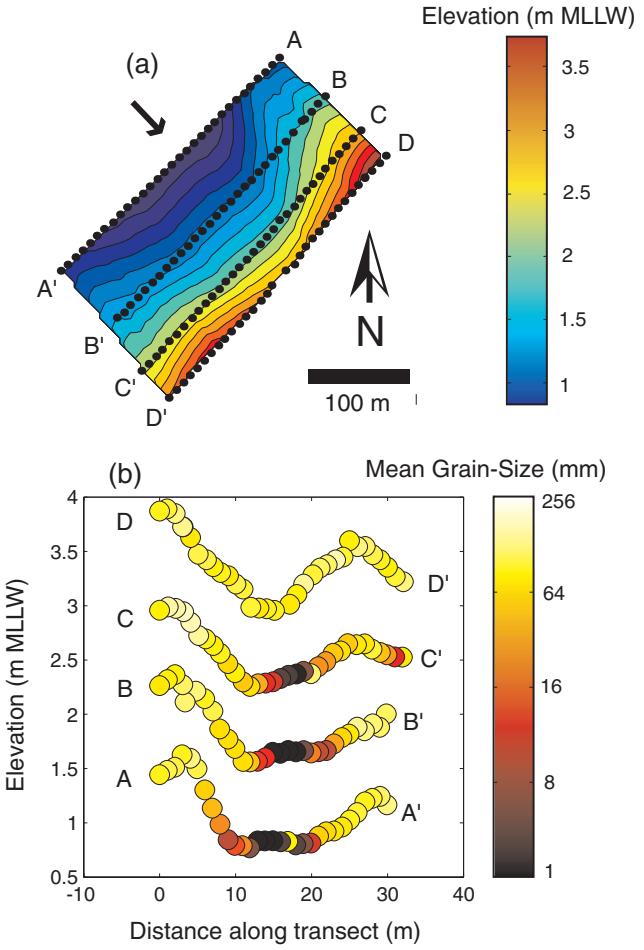

Figure 13. Example topography (a) and mean grain size (b) along four transects representing 128 samples of a beach cusp along the Elwha River delta beach. Perspective in (b) is shown with a black arrow in (a). An oblique photograph of transect B–B′ is shown in Figure 1c.

Rather than generate unique calibration curves for the Kachemak site, we tested the applicability of the Elwha River calibration curves to the Kachemak Bay images. Surprisingly, the autocorrelation algorithm showed remarkable agreement with photo-based size measurements, although with a systematic overestimation ($r^2 = 0{\cdot}97$; slope = 1·35; mean error = 21%; Figure 15). Correcting the r.m.s.e. (26%) for the effect of this overestimation with equation [4], we found that the irreducible error of the prediction was only 16%, which is consistent with the general technique described above (cf. Figure 8). Thus, any additional samples obtained during this field exercise could be corrected for this overprediction using the statistics shown in Figure 15. This example shows that the autocorrelation technique and calibration curves may be transferable from one location to another, although only following the measurement and correction for systematic errors as shown in the example above. These errors can be evaluated with simple photo-based, grid-by-number counts of the grain sizes on a limited number of images.

Discussion and conclusion

It has been shown here that the photographic autocorrelation technique can be applied to grain size assessments of mixed sand and gravel settings, which is a significant advancement over the sand or gravel only analyses currently employed (Rubin, 2004; Barnard *et al.*, 2007; Buscombe and Masselink, 2009). Uncertainty in the method presented here (error = 14%)

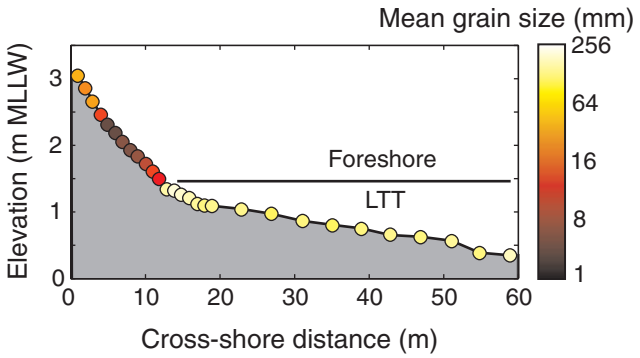

Figure 14. Example topography and mean grain size along an across–shore transect of 30 samples of a foreshore to low–tide terrace (LTT) transition along the Elwha River delta beach. An oblique photograph of the region of this transect is shown in Figure 1d.

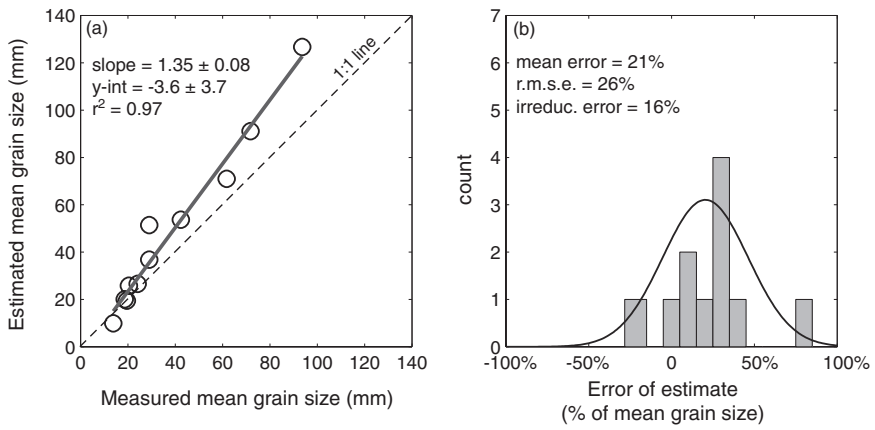

Figure 15. Comparison of the measured and estimated mean grain size for the mixed sediment beaches of Kachemak Bay, Alaska using the autocorrelation algorithms developed for the Elwha River delta beaches. (a) Comparison with linear regression statistics, (b) histogram of the error of the estimates. Solid line in (b) is a normal distribution calculated with estimate errors.

Copyright © 2009 John Wiley & Sons, Ltd.

DOI: 10.1002/esp

is consistent with the methods designed for sand, and we show that this level of uncertainty is acceptable for characterizing the coastal landforms considered here (Figures 13 and 14). We also suggest that a significant level of uncertainty – approximately half – arose from the use of ambient solar illumination during our data collection. There is also the potential for significant mean errors in application of this method, such as shown with independent investigations of the effects of solar zenith angle on directly illuminated imagery and partial wetted sediment. These effects may be accounted for if they are continuous within any field site, or portion thereof, with simple linear-based corrections from photo-based measurements.

Our errors are compared with those shown for the object-detection methods of Graham *et al*. (2005a) in Table I. Unfortunately, we cannot compare directly with the results presented above, because Graham *et al*. (2005a) only provide log-transformed error analyses. However, if our errors are recomputed from log-transformed data, it can be shown that they are significantly less than the Graham *et al*. (2005a) errors in both ambient and controlled lighting conditions (Table I). Further, it is noted that the autocorrelation method can be applied over a larger range of grain sizes without the need to modify the camera set-up. Reported range in D_{50} of the edge and object-detection methods is about 5–6 fold, or ~2·5ϕ, whereas we show here that the autocorrelation method can be applied to a range of mean grain sizes extending at least 200-fold, or ~7·5ϕ (Table I). A significant limitation of the technique presented in this paper is the lack of good grain size distribution estimates that can be provided by object-detection methods. In light of this, a valuable contribution from future work will be the evaluation of grain size distribution properties using the modified autocorrelation techniques of Buscombe (2008). We have, however, shown here that the standard error of the series of estimates for any one sample is related to grain size sorting, which is a considerable step closer to characterizing grain size distributions. Future programs to assess grain size will need to carefully consider these strengths and limitations to arrive at methods and results that are of adequate quality for the research or monitoring needs.

With this in mind, we suggest that the autocorrelation technique has strong potential for successful application to other mixed sediment inventories in the future. In fact, our findings that the calibration curves were closely equivalent to exponential functions and could be effectively applied from one site (Elwha, Washington) to another (Kachemak, Alaska) with simple scaling factors and low uncertainty suggests that these techniques may be broadly applicable to mixed-sediment settings. For this reason, we term the general technique 'cobble cam'. Future application of the cobble cam technique should include consistent control of the illumination of the photographs with at least shading and perhaps flash. Having control over illumination will be especially important where shadows may be cast upon the ground surface from features such as foliage. If illumination can be well controlled, uncertainty in the method may drop by up to half from that reported in Figure 8. Adequate calibration information for additional sites should be available from grid-by-number sediment counts on a subset of the images.

The cobble cam technique appears to be valuable for rapid grain size assessments of plots of ground surface. It will probably be impractical to use the cobble cam method to evaluate grain size patterns over multiple kilometer length scale features, however. Under such scenarios, the cobble cam method may provide excellent calibration data for aerial remote sensing techniques such as those used by Carbonneau *et al*. (2004) or Verdu *et al*. (2005).

Note that significant advancement could be made if the technique could be brought underwater to characterize streambeds or the ocean floor. There are already operational techniques for underwater sand photography (Chezar and Rubin, 2004; Rubin *et al*., 2007), but such a technique for gravel may be challenging especially if water is not at sufficient depth to obtain an adequate field of view or if the water is too turbid to observe the bed.

Table I. Comparison of automated grain-size methods on a grid-by-number basis

	1	2	3	4	5
	Range of particle sizes	Type of result	Percentage error calculated from grain sizes in mm (linear scale)*	Error calculated from grain sizes in phi (log scale)*	Percentage error equivalent of errors in column 4 ***
This paper – ambient lighting	1 – 200 mm (mean grain size); factor of 200	Mean of all grains coarser than 2–3 pixels.	14%	0·18 phi	14%
This paper – controlled lighting	Not evaluated	Mean of all grains coarser than 2–3 pixels.	~7%##	~0·09 phi##	~7%
Graham et al. (2005) – ambient lighting	Not evaluated	Percentiles of all grains coarser than 23 pixels.	Not evaluated	0·5 – 1·3 phi#	40–250%
Graham et al. (2005) – controlled lighting	16 – 90 mm** (median grain size); factor of 6	Percentiles of all grains coarser than 23 pixels.	Not evaluated	0·18 phi	13%

* Error values reported are bias-corrected r.m.s. errors of either the grain-size mean (this paper) or median (Graham et al., 2005).
\# Graham et al. (2005) report that irreducible random errors increased by between 3 and 7 times for photographs obtained in sunlight and without an overhead flash. Values shown in this table are their results multiplied by this factor.
** Obtained from Figure 5 of Graham et al. (2005).
\## Reduction of error associated with controlled lighting is approximated to be a factor of 2 based on the results presented in Figure 12.
*** For consistency, we converted the phi values (α) in column 4 to percentages (ρ) in column 5, using the following equation: $\rho = 2^{\alpha}$.

Copyright © 2009 John Wiley & Sons, Ltd.

DOI: 10.1002/esp

In conclusion, the autocorrelation method has been extended to include gravel and boulder-size sediment by using a simple digital camera. Although the method was successfully developed with uncertainty levels adequate to characterize the coastal features of interest here, there may be ways to improve upon these results especially by consistently controlling illumination. For future applications of the cobble cam method, the coding used in these analyses is provided on the lead author's USGS professional webpage (http://walrus.wr.usgs.gov/staff/jwarrick/).

Acknowledgements—We would like to thank the Lower Elwha Klallam Tribe for access to the Elwha River delta and for their support of this research. Field assistance was provided by Doug George, Katie Farnsworth, Andrew Stevens and Guy Gelfenbaum. Computer coding assistance was provided by Erin Todd and Josh Logan. Sarah McNaboe, Melinda Garvey and Liron Friedman assisted with digital grain-size counts and analyses. Bruce Richmond and Eric Grossman provided helpful comments on an earlier draft of this paper. Two anonymous reviewers and the editors of ESPL helped shape this final version of the paper. The use and description of specific equipment, software, and/or brand names in this paper does not in any way imply an endorsement by the US Geological Survey or the US Department of Interior. This work was funded by the USGS Coastal and Marine Geology Program and the USGS Coastal Habitats in Puget Sound (CHIPS) program.

References

Adams J. 1979. Gravel size analysis from photographs. *ASCE Journal of the Hydraulics Division* **105**(10): 1247–1255.

Adams PN, RuggieroP, Schoch GC, Gelfenbaum G. 2007. Intertidal sand body migration along a megatidal coast, Kachemak Bay, Alaska. *Journal of Geophysical Research* **112**, F02007, doi:10.1029/2006JF000487.

Barnard PL, Rubin DM, Harney J, Mustain N. 2007. Field test of an autocorrelation technique for determining grain size using a digital 'beachball' camera versus traditional methods. *Sedimentary Geology* **201**: 180–195.

Buscombe D. 2008, Estimation of grain-size distributions and associated parameters from digital images of sediment. *Sedimentary Geology* **210**: 1–10, doi: 10.1016/j.sedgeo.2008.06.007

Buscombe D, Masselink G. 2006, Concepts in gravel beach dynamics: *Earth–Science Reviews* **79**: 33–52.

Buscombe D, Masselink G. 2009, Grain-size information from statistical properties of digital images of sediment. *Sedimentology* **56**: 421–438, doi: 10.1111/j.1365–3091.2008.00977.x

Butler JB, Lane SN, Chandler JH. 2001, Automated extraction of grain–size from gravel surfaces using digital image processing, *Journal of Hydraulic Research* **39**: 519–529.

Carbonneau PE, Lane SN, Bergeron NE. 2004, Catchment-scale mapping of surface grain size in gravel bed rivers using airborne digital imagery. *Water Resources Reseach* **40**, W07202.

Chezar, H., Rubin, D.M., 2004. Underwater Microscope System. United States Patent Office, The United States of America as represented by the Secretary of the Interior, US Patent No. 6,680,795 B2.

Church MA, DG McLean, JF Wolcott. 1987. River bed gravels: sampling and analysis. In *Sediment Transport in Gravel-bed Rivers,* Thorne CR, Bathurst JC, Hey RD (eds). John Wiley & Sons: Chichester; 43–78.

Finkl CW. 2004, Coastal classification: system approaches to consider in the development of a comprehensive scheme. *Journal of Coastal Research* **20**: 166–213.

Gomez B. 1983, Temporal variations in bedload transport rates: the effect of progressive bed armoring. *Earth Surface Processes and Landforms* **8**: 41–54.

Graham DJ, Rice SP, Reid I. 2005a. A transferable method for the automated grain sizing of river gravels. *Water Resources Research* **41**, W07020, doi:10.1029/2004WR003868.

Graham DJ, Reid I, Rice SP. 2005b Automated sizing of coarse–grained sediments: image processing procedures. *Mathematical Geology* **37**: 1–28.

Ibbeken H, Schleyer R. 1986, Photo-sieving: a method for grain-size analysis of coarse-grained, unconsolidated bedding surfaces. *Earth Surface Processes and Landforms* **11**: 59–77.

Iriondo M. 1972, A rapid method for size analysis of coarse sediments. *Journal of Sedimentary Petrology* **42**: 985–986.

Kellerhals R, Bray DI. 1971. Sampling procedures for coarse fluvial sediments. *ASCE Journal of the Hydraulics Division* **97**: 1165–1179.

Klingeman PC, Emmett WW. 1982, Gravel bedload transport processes. In *Gravel Bed Rivers*, Hey RD, Bathurst JC, Thorne CR (eds). Wiley: Chichester; 141–179.

Leopold LB. 1970. An improved method for size distribution of stream bed gravel. *Water Resources Research* **6**: 1357–1366.

Mason T, Coates TT. 2001, Sediment transport processes on mixed beaches: a review for shoreline management. *Journal of Coastal Research* **17**: 645–657.

Randle TJ, Young CA, Melena JT, Ouellette EM. 1996. Sediment analysis and modeling of the river erosion alternative. Elwha Technical Series PN–95–9, U.S. Department of the Interior, Bureau of Reclamation, Boise, ID.

Rubin DM. 2004. A simple autocorrelation algorithm for determining grain size from digital images of sediment. *Journal of Sedimentary Research* **74**: 160–165.

Rubin DM, Chezar H, Harney JN, Topping DJ, Melis TS, Sherwood CR. 2007. Underwater microscope for measuring spatial and temporal changes in bed-sediment grain size. In *From Particle Size to Sediment Dynamics, Sedimentary Geology*, Vol. 202, Hartmann D, Flemming BW (eds) Elsevier: The Netherlands; 402–408.

Rubin DM, Topping DJ. 2001. Quantifying the relative importance of flow regulation and grain-size regulation of suspended-sediment transport (a) and tracking changes in grain size on the bed (b). *Water Resources Research* **37**: 133–146.

Ruggiero P, Adams P, Warrick J. 2007. Mixed sediment beach processes: Kachemak Bay Alaska, 2007. In *Proceedings Coastal Sediments 2007*. ASCE: New Orleans, LA.

Sedimetrics. 2008. Sedimetrics Digital Gravelometer documentation (version 1.0), available at: http://www.sedimetrics.com/documentation/introduction.html (accessed July 1, 2008).

Sime LC, Ferguson RI. 2003. Information of grain sizes in gravel–bed rivers by automated image analysis. *Journal of Sedimentary Research* **73**(4): 630–636.

Verdu JM, Batalla RJ, Martinez-Casanovas JA. 2005. High-resolution grain-size characterization of gravel bars using imagery analysis and geo-statistics. *Geomorphology* **72**: 73–93.

Warrick JA, George DA, Stevens AW, Eshleman J, Gelfenbaum G, Kaminsky GM, Schwartz AK, Bierne M. 2007. Beach morphology monitoring in the Elwha River littoral cell, 2004–2006. US Geological Survey, Data Series 288, and data folder [http://pubs.usgs.gov/ds/288/].

Warrick JA, George DA, Gelfenbaum G, Ruggiero P, Kaminsky G, Beirne M. 2009. Beach morphology and change along the mixed grain size delta of the Elwha River, Washington, *Geomorphology* **111**: 136–148.

Wolman MG. 1954. A method of sampling coarse river-bed material. *Transactions American Geophysical Union* **35**: 951–956.

Copyright © 2009 John Wiley & Sons, Ltd.